

Observation of Polarization of the Soft X-Ray Laser Line in Neonlike Germanium Ions

T. Kawachi,^{1,*} K. Murai,^{2,†} G. Yuan,^{2,‡} S. Ninomiya,² R. Kodama,² H. Daido,² Y. Kato,² and T. Fujimoto¹

¹Department of Engineering Science, Kyoto University, Kyoto 606-01, Japan

²Institute of Laser Engineering, Osaka University, Suita, Osaka 565, Japan

(Received 25 October 1994; revised manuscript received 7 June 1995)

A 3-cm-long curved Ge slab target was irradiated by 1.053 μm glass laser light with irradiance of $2.9 \times 10^3 \text{ W/cm}^2$. The 19.6 nm laser line due to the $3p \rightarrow 3s, J = 0 \rightarrow 1$ transition in Ne-like Ge ions was found to be polarized parallel to the target surface, with a degree of polarization of $\sim 53\%$. This polarization is accounted for by the anisotropy in the radiation trapping of the resonance line in an expanding plasma, which has a velocity gradient in the direction normal to the target surface.

PACS numbers: 42.55.Vc

Since the demonstration of soft x-ray amplification [1,2], continuing efforts have been directed toward the development of high-performance x-ray lasers. It is now possible to conduct plasma diagnostic experiments by using high brightness collisional excitation x-ray lasers [3]. Based on advanced modeling, we are now able to analyze quantitatively the performance of these lasers, including the collisional excitation, Ne-like Ge x-ray laser [4]. However, even for this well-studied laser, there still remain discrepancies between theory and experiment. For example, the gain of the 19.6 nm line due to the $3p \rightarrow 3s, J = 0 \rightarrow 1$ transition [the transition from $(2p_{1/2}, 3p_{1/2})_0$ to $(2p_{1/2}, 3s_{1/2})_1$] is predicted to be $\sim 12 \text{ cm}^{-1}$, much higher than experimental results.

One phenomenon that has attracted little attention so far is the spatial anisotropy of the plasma and the resulting polarized emission. Kieffer *et al.* observed polarized x-ray emission from an Al plasma produced by a 1 ps laser pulse [5]. They interpreted this polarization as due to the spatial anisotropy in the velocity distribution of the plasma electrons. In soft x-ray laser experiments, polarized radiation has been generated with the Ge laser by double-pass amplification by use of a half cavity in which an oblique incidence multilayer mirror was used as a polarizer [6,7]. However, Rus *et al.* [7] found no polarization in the original 23.2 and 23.6 nm laser lines where a slab target was irradiated with a 650 ps pulse of 1 μm wavelength at $1.6 \times 10^3 \text{ W/cm}^2$ intensity; the upper bound of the degree of polarization was $(4 \pm 2)\%$.

In the following we report the first observation of the existence of polarization of the 19.6 nm Ne-like Ge laser line generated without polarization seeding.

Figure 1 shows the experimental setup. Soft x-ray amplification was obtained with a curved slab target of Ge where a 1- μm -thick, 200- μm -wide Ge stripe was coated on a glass plate of 3 cm length that was bent cylindrically with a 2.5 m radius of curvature [8]. One beam of the GEKKO XII Nd:glass laser (1.053 μm), linearly polarized counterclockwise 14.5° with respect to the y direction, irradiated the target from the z direction. A cylindrical lens and an aspherical lens produced a line

focus on the target along the y axis of 6 cm length and 100 μm average width [9]. The laser light consisted of two Gaussian pulses of 0.1 ns width separated by 0.4 ns. X-ray amplification was observed at the second irradiation pulse. This double pulse excitation was effective in enhancing the 19.6 nm output [10]. The total energy on the 3 cm length target was either 170 or 190 J, at which the average irradiance of the second pulse was $2.9 \times 10^{13} \text{ W/cm}^2$ or $3.2 \times 10^{13} \text{ W/cm}^2$, respectively.

The x-ray laser light was observed in the y direction by a high resolution spectrometer (HI REFS) [11]. The distance between the entrance slit and the grating G was 134 cm and that from the grating to the focal plane was 409 cm. The output end of the x-ray laser was located at 8.5 cm in front of the entrance slit, which was removed in this experiment in order to minimize the shot-to-shot fluctuation in the transmittance through the slit. The laser beam was first reflected by a concave mirror M1, dispersed along the vertical (x) direction by an unevenly spaced grating of 375 lines/mm and then reflected by a cylindrical mirror M2 to be weakly focused along the z direction. The length of the spectral lines along the z direction was approximately 1.5 cm in the recording plane. The linear reciprocal dispersion was 0.6 nm/mm.

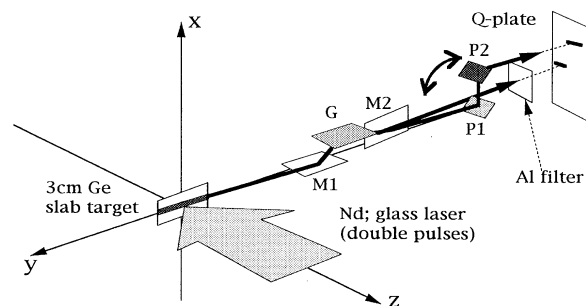


FIG. 1. Nd:glass laser irradiates along the z direction a slab target and the 19.6 nm line is amplified along the y direction. M1: concave mirror; M2: cylindrical mirror; G: grating; P1 and P2: polarizer. The beam passing by the side of P1 is for intensity monitor.

The central 0.6 cm portion of the 19.6 nm laser line was passed through a reflective linear polarizer placed at about 20 cm in front of the recording plane. The polarizer consisted of two square shaped (1 cm \times 1 cm) Mo/Si multilayer mirrors, which were positioned parallel to each other. The two mirrors were fixed in a housing that was rotated around the optical axis in measuring the x-ray intensities with different polarization directions. The angle of incidence of the xuv radiation to these mirrors was 38° with respect to their surface normal. A possible deviation in the angle of incidence caused by inaccurate rotation of the polarizer was less than 10 mrad. These mirrors were calibrated with synchrotron radiation. The reflectivity R_s for the radiation polarized in the direction perpendicular to the incident plane was measured to be about 25% at 19.6 nm, and the polarization efficiency R_s/R_p was estimated to be >100 for each mirror [5]. The output radiation from the polarizer was displaced by 1.0 cm in the incidence plane of the mirrors.

An Ilford Q plate was used for recording the spectra. This plate was located at the original focal plane. Although the spectra were slightly off focus due to the increase in the optical path of 1.0 cm in the polarizer together with the 8.5 cm axial displacement of the light source from the entrance slit position, the actual increase in the spectral width of the laser line was negligible. The photometric response (optical density versus exposure) of the Q plate was calibrated by use of a carbon plasma produced by a Nd:YAG laser of 8 ns pulse, illuminating normally a carbon plate with a spot focus. The C VI $H\alpha$ line at 18.2 nm was observed at 45° with respect to the surface normal. The relative transmittance of the spectrometer to the radiation with different polarizations was determined by using the carbon line and a continuum at 19.6 nm from an aluminum plasma produced similarly. The absence of polarization in these spontaneous emissions was confirmed using an arrangement similar to that described in Ref. [12]. A relative transmittance S_{\parallel}/S_{\perp} of 1.3 ± 0.1 was obtained, where \parallel and \perp stand, respectively, for the polarization direction parallel and perpendicular to the z direction. No wavelength dependence of S_{\parallel}/S_{\perp} was detected.

In measuring the polarization of the x-ray laser beam, the 19.6 nm laser line was first recorded without the polarizer [Fig. 2(a)]. We then placed the polarizer at the central portion of the spectrum and recorded the intensity shot by shot with the polarization axis set in the direction parallel (\parallel), perpendicular (\perp), and 45° to the z axis. Figure 2(b) shows the plates corresponding to the polarized components together with their densitometer traces scanned over the spectral line. A portion of the 19.6 nm laser line, which went by the side of the first polarizer mirror and transmitted through a 1.47 μm thick Al filter, was used to monitor the reproducibility of the shots. This "monitored intensity" I_{mon} was used to derive the normalized relative intensities $I_{\parallel}/I_{\text{mon}}$, I_{\perp}/I_{mon} , and $I_{45^\circ}/I_{\text{mon}}$, where the correction for S_{\parallel}/S_{\perp} has been made for the observed intensities.

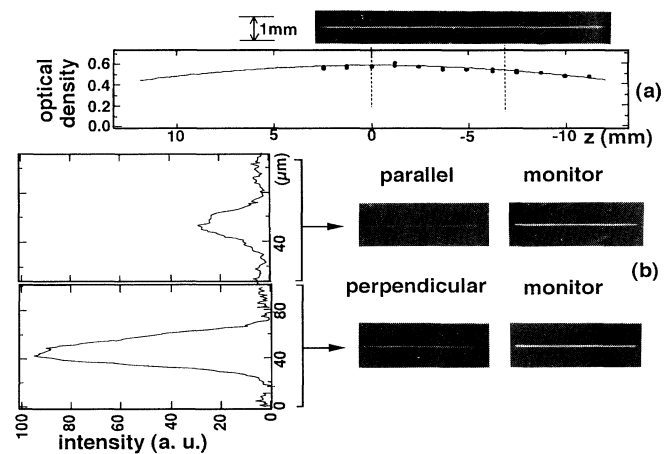


FIG. 2. (a) The 19.6 nm laser spectrum recorded with the polarizer removed and its optical density at the peak, where z is the position along the z axis. (b) Images of the polarized components and their densitometer traces that correspond to the portion of the spectral line indicated with the dotted line in (a). Images of the intensity monitor are also shown.

Table I shows two sets of data with different irradiation laser energies: 170 J for the first three shots and 190 J for the last two shots. The gain depends strongly on the irradiance of the second laser pulse, whose energy is shown by the second figure in the parentheses. Approximately 20% increase in the second pulse energy results in ~ 2 times increase in the x-ray laser energy (I_{mon}), which corresponds to $\sim 10\%$ increase in the gain for the 2.7 cm^{-1} gain and 3 cm gain length. This may be ascribed mainly to an increase in the electron temperature (T_e).

The intensity ratio defined as $[I_{\parallel}/I_{\text{mon}}]/[I_{\perp}/I_{\text{mon}}]$ is 3.3 for the 170 J shots and 1.5 for the 190 J shots. The experimental results show that the 19.6 nm laser line is polarized along the target surface with the degree of polarization $P = (I_{\parallel} - I_{\perp})/(I_{\parallel} + I_{\perp})$ of -0.53 and -0.19 for the 170 and 190 J shots, respectively. The experimental uncertainty in the measured x-ray laser energy was estimated to be 11%, which is due to the calibration error of the spectrometer (7.7%), the deviation in the angle of incidence of the polarizer (4.5%), and the reading error of the densitometer trace (5%). In the 170 J shots, the $I_{45^\circ}/I_{\text{mon}}$ is predicted to be $(I_{\parallel}/I_{\text{mon}} + I_{\perp}/I_{\text{mon}})/2 = 0.29$, in agreement with the experimental value.

The spontaneous emission of the 19.6 nm line ($J = 0 \rightarrow 1$) is never polarized. (Ge has virtually no nuclear spin. See also Fig. 3.) The possible existence of polarization due to the superradiance [13,14] should be excluded, since the plasma size is far larger than the correlation length between the atoms and, if superradiance sets in, the polarization direction should vary from shot to shot [14], contrary to the present experimental results. Thus, we conclude that the difference in the intensities of the polarized components of the laser output is due solely

TABLE I. Relative intensities of the linearly polarized components of the 19.6 nm laser line, normalized by the monitored intensity. The gain (target) length is 3 cm.

Energy	Monitored intensity I_{mon}	Intensity of polarized components	Normalized intensity I/I_{mon}
169 J = (84 + 85)	7.3	Parallel (I_{\parallel}) = 1	0.14 ± 0.03
171 J = (83 + 88)	7.4	Perpendicular (I_{\perp}) = 3.3	0.45 ± 0.08
164 J = (82 + 82)	7.1	45° (I_{45}) = 1.9	0.27 ± 0.05
195 J = (92 + 103)	14.9	$I_{\parallel} = 4.1$	0.28 ± 0.04
187 J = (87 + 100)	15.3	$I_{\perp} = 6.0$	0.39 ± 0.05

to a difference in the gains of these components. Let g_{\parallel} and g_{\perp} denote the gains for the parallel and perpendicular components, respectively. We take the 170 J shots as an example. The intensity ratio 3.3 indicates the difference in the gains to be $g_{\parallel} - g_{\perp} = -0.5 \pm 0.1 \text{ cm}^{-1}$. Let M be the projection of J ($= 1$ for $3s$) onto the quantization axis, z axis, and $n(3s)_M$ be the population of the magnetic sublevel M . We note the relationship $g_{\parallel} \propto [n(3p) - n(3s)_0]$ and $g_{\perp} \propto [n(3p) - n(3s)_{\pm 1}]$ (Fig. 3). Our experimental result indicates that $n(3s)_0$ is larger than $n(3s)_{\pm 1}$, or the $3s$ level ions have negative alignment.

Analysis of our previous experimental results [10] for the transient behavior of amplification shows that the gain for the 19.6 nm line is approximately 2.7 cm^{-1} . This value is regarded as the average over the two polarization components. From the observed intensity ratio, g_{\parallel} and g_{\perp} were evaluated to be 2.4 and 2.9 cm^{-1} , respectively. We assume that the gain profile is given by a Voigt profile determined by the thermal Gaussian width $\Delta\omega_G = 8.8 \times 10^{12} \text{ s}^{-1}$ (FWHM for the ion temperature of $T_i = 100 \text{ eV}$) and the natural width $\Delta\omega_L = 1.7 \times 10^{12} \text{ s}^{-1}$ ($2 \times 10^{10} \text{ s}^{-1}$ for $3p$ and $1.7 \times 10^{12} \text{ s}^{-1}$ for $3s$) [15]. The Stark width is $3 \times 10^{10} \text{ s}^{-1}$; see below. It then follows that $[n(3p) - n(3s)_{\pm 1}] = 1.4 \times 10^{15} \text{ cm}^{-3}$, $[n(3p) - n(3s)_0] = 1.2 \times 10^{15} \text{ cm}^{-3}$.

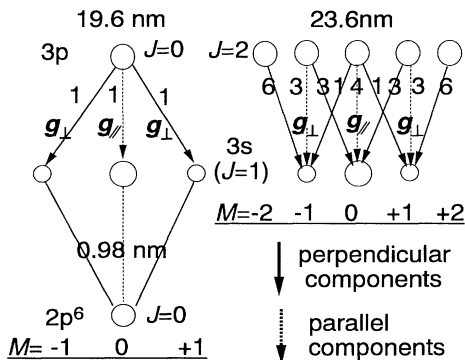


FIG. 3. Kastler diagram for the 19.6 nm, 23.6 nm laser transitions and the 0.98 nm resonance transition. M is the magnetic quantum number. Solid and dotted arrows indicate the perpendicular and parallel components of the polarized emission, respectively. The number on the arrows shows the relative transition probability.

The $3s$ population is estimated as follows: The $3s$ level has a large radiative decay rate into the ground state, and corona equilibrium is approximately established for this level. The hydrodynamics simulation [16] shows that, in the gain region, T_e , n_e , T_i , and Ne-like Ge ground-state density are 600 eV, $1 \times 10^{20} \text{ cm}^{-3}$, 100 eV, and $3 \times 10^{18} \text{ cm}^{-3}$, respectively. Since the excitation rate coefficient from the ground state is $6.1 \times 10^{-13} \text{ cm}^3 \text{ s}^{-1}$ [17], the $n(3s)$ is estimated to be $4 \times 10^{14} \text{ cm}^{-3}$, where the reduced spontaneous transition probability by a factor 3.6 has been used, which is due to a slight radiation trapping effect as explained later. Since the uncertainty in n_e , T_e , and atomic parameters is about 50%, the uncertainty of $n(3s)$ is at least a factor of 2. It readily follows that $n(3p) = 1.5 \times 10^{15} \text{ cm}^{-3}$, $n(3s)_0 = 2.6 \times 10^{14} \text{ cm}^{-3}$, and $n(3s)_{\pm 1} = 0.7 \times 10^{14} \text{ cm}^{-3}$. The population imbalance of $3s$, defined as $[n(3s)_0 - n(3s)_{\pm 1}]/n(3s)$, is 0.5.

Since our plasma was produced by a relatively long laser pulse, spatial anisotropy in the velocity distribution of electrons is unlikely to develop, and the above alignment cannot be ascribed to anisotropic collisions [5]. Instead, radiation trapping of the 0.98 nm resonance line due to $3s \rightarrow 2p^6$ ($J = 1 \rightarrow 0$) transition could create alignment in the $3s$ level ions. The hydrodynamics simulation [16] shows that our plasma has a streaming motion dominantly in the z direction, resulting in a velocity gradient of $1 \times 10^7 \text{ cm/s}$ per $100 \mu\text{m}$. Under such a plasma condition, the absorption spectrum of ions in the laboratory coordinate system is shifted with their z position due to the Doppler effect. This could reduce the absorption of photons of the resonance transition emitted in the z direction as compared with those in the x direction; i.e., the number of the dipoles oscillating in the x direction ($M = \pm 1$ levels) tends to decay faster than that in the z direction ($M = 0$ level). Alignment created by anisotropic radiation trapping was first treated analytically [18], and recently using a Monte Carlo simulation code [19]. We have modified this code and applied it to the present case with the disalignment process included.

The Stark broadening was estimated by use of the impact approximation [20], and the corresponding rate was used as an estimate of the disalignment [21]; it is $1.5 \times 10^{10} \text{ s}^{-1}$. (It is $3 \times 10^{10} \text{ s}^{-1}$ for the laser line.)

It should be noted that the electron-ion elastic collisions, of the order of 10^{14} s^{-1} , do not contribute to Stark broadening and thus to disalignment [22]. We assume the dimension of the plasma to be $100 \mu\text{m}$ in the z direction and $60 \mu\text{m}$ in the x direction with a velocity gradient 10^7 cm/s per $100 \mu\text{m}$ only in the z direction. We assume the absorption profile of the resonance line to be a Voigt profile ($\Delta\omega_G = 1.8 \times 10^{14} \text{ s}^{-1}$ and $\Delta\omega_L = 1.7 \times 10^{12} \text{ s}^{-1}$) and the complete frequency redistribution.

First a dipole is created at a location randomly chosen from an appropriate probability function. After a certain time determined by the natural lifetime of the $3s \rightarrow 2p^6$ ($J = 1 \rightarrow 0$) transition 0.59 ps , the ion emits a photon in a direction in the plane determined by the oscillating direction. Disalignment may occur in the time interval, in which case a new oscillating direction of the electric dipole is randomly given. The emitted photon is absorbed after a space interval and produces another dipole oscillating in the direction that is determined by the oscillating direction of the original dipole and the photon propagating direction. The direction of the oscillating dipole is "quantized" into one of the x , y , and z directions. This procedure is repeated until the last photon escapes from the plasma. We repeat the similar series of procedures 6×10^4 times and count at each time after the start the number of the dipoles oscillating in a certain direction. We find that, after several lifetimes, the decay time constant of the total number of dipoles or $n(3s)$ reaches its final constant value of 2.1 ps ; i.e., the escape factor is $0.59/2.1 = 1/3.6$. We also find the imbalance of $3s$ to be 0.26 . In view of many simplifications made above, the disagreement between the calculated (0.26) and the experimental (0.5) values of the population imbalance may not be regarded to be serious. For the 190 J shots, the experimental population imbalance in $3s$ is 0.2 . The increase in the irradiance leads to an increase in n_e and T_i , which may result in the decrease in the population imbalance: The increased n_e enhances the disalignment and the increased T_i causes the broadening of the absorption profile, which makes the plasma optically more isotropic. For more quantitative analysis, a multidimensional hydrodynamics simulation coupled with a collisional-radiative model is needed.

We estimate the polarization degree of the $J = 2 \rightarrow 1$ 23.6 nm line, which shares the same lower level with the 19.6 nm line, under the same plasma condition. We

assume that the upper level is unpolarized and that the gains of the transitions terminating on the $M = 0$ and ± 1 levels are equal to g_{\parallel} and g_{\perp} , respectively, of the 19.6 nm line. From the Kastler diagram for the $J = 2 \rightarrow 1$ line (Fig. 3), the relative gains of the perpendicular and parallel components are $[(6 + 1)g_{\perp} + 3g_{\parallel}]/10$ and $[(3 + 3)g_{\perp} + 4g_{\parallel}]/10$, respectively, from which the polarization degree of the output is estimated to be 8% .

*Present address: The Institute of Physical and Chemical Research, Saitama 351, Japan.

†Present address: Osaka National Research Institute, AIST, Ikeda 563, Japan.

‡Present address: Shock Dynamic Center, Washington State University, Pullman, WA 99164-2814.

- [1] D.L. Matthews *et al.*, Phys. Rev. Lett. **54**, 110 (1985).
- [2] S. Suckewer *et al.*, Phys. Rev. Lett. **55**, 1753 (1985).
- [3] L.B. DaSilva *et al.*, Proc. SPIE Int. Soc. Opt. Eng. **2012**, 158 (1993).
- [4] P.B. Holden *et al.*, J. Phys. B **27**, 341 (1994).
- [5] J.C. Kieffer *et al.*, Phys. Rev. E **48**, 4648 (1994).
- [6] K. Murai *et al.*, Jpn. J. Appl. Phys. **33**, L600 (1994).
- [7] B. Rus *et al.*, Phys. Rev. A **51**, 2316 (1995).
- [8] R. Kodama *et al.*, Phys. Rev. Lett. **73**, 3215 (1994).
- [9] K. Murai *et al.*, J. Opt. Soc. Am. (to be published).
- [10] H. Daido *et al.*, Opt. Lett. **20**, 61 (1995).
- [11] M.C. Hettrick *et al.*, Appl. Opt. **27**, 200 (1988).
- [12] S. Nakayama *et al.*, Phys. Scr. **41**, 754 (1990).
- [13] A. Crubellier *et al.*, J. Phys. B **19**, 2959 (1986).
- [14] A. Sureau, *X-ray Lasers 1992* (IOP, London, 1992), p. 251.
- [15] M. Cornille *et al.*, At. Data Nucl. Data Tables **58**, 1 (1994).
- [16] H. Takabe, J. Quant. Spectrosc. Radiat. Transfer **51**, 379 (1994).
- [17] D.H. Sampson and H.L. Zhang, At. Data Nucl. Data Tables **43**, 1 (1986).
- [18] V.I. Perel' and V.I. Rogova, Sov. Phys. JETP **34**, 965 (1972); **38**, 501 (1974).
- [19] A. Hishikawa *et al.*, Phys. Rev. A **52**, 189 (1995).
- [20] I.I. Sobelmann *et al.*, *Excitation of Atoms and Broadening of Spectra* (Springer-Verlag, Berlin, 1981).
- [21] A. Hirabayashi *et al.*, Phys. Rev. A **37**, 83 (1988).
- [22] H.R. Griem, in Proceedings of the 9th International Conference on Spectral Line Shapes, Poland, 1988 (unpublished).

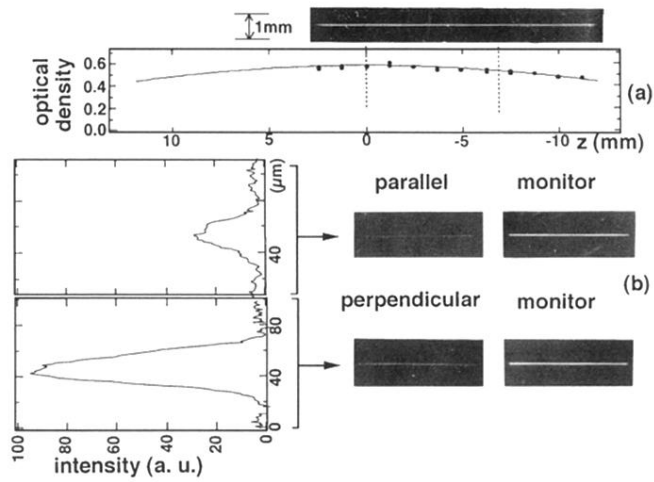


FIG. 2. (a) The 19.6 nm laser spectrum recorded with the polarizer removed and its optical density at the peak, where z is the position along the z axis. (b) Images of the polarized components and their densitometer traces that correspond to the portion of the spectral line indicated with the dotted line in (a). Images of the intensity monitor are also shown.